Study on the Role of Stearic Acid and Ethylene-bis-stearamide on the Mechanical Alloying of a Biomedical Titanium Based Alloy

ALIREZA NOURI, PETER D. HODGSON, and CUI'E WEN

The present study examines the influence of different contents and types of process control agent (PCA), *i.e.*, stearic acid (SA) and ethylene-bis-stearamide (EBS), on the microstructural evolution and characteristics of Ti-16Sn-4Nb (wt pct) alloy powders and bulk samples. The characterization of the powders and bulk samples was carried out by using chemical analysis, optical microscopy, scanning electron microscopy (SEM) combined with energy-dispersive spectrometry (EDS), and X-ray diffractometry. Results indicated that the powder recovered from the ball milling containers increased with increasing amounts of SA and EBS. Furthermore, adding more SA or EBS to the powder mixture resulted in a considerably smaller particle size, with a flaky-shaped morphology for the given ball milling time. Also, a slightly higher effectiveness was found for EBS when compared to SA. Meanwhile, the addition of both SA and EBS led to a delay in the alloy formation during mechanical alloying (MA) and caused contamination of the material with mainly carbon (C) and oxygen (O). An optimum amount of 1 wt pct PCA led to a good balance between cold welding and fracturing, and thus favored the formation of the titanium alloy. The microstructural observation of the bulk alloy showed a homogeneous distribution of fine Nb-rich β-phase colonies within the α-Ti matrix with the addition of PCA less than 1 wt pct.

DOI: 10.1007/s11661-010-0207-5

I. INTRODUCTION

MECHANICAL ALLOYING (MA) is a powder processing technique, in which initial elemental metal powders are continuously impacted by high energy balls in a container. MA is capable of synthesizing a variety of equilibrium and nonequilibrium materials including supersaturated solid solutions, amorphous metals and alloys, as well as nanostructural and quasicrystalline phases.[1,2] It is also used to produce several alloys and compounds that are difficult or impossible to be obtained by the conventional ingot melting techniques.[3] Interest in MA has been constantly growing for synthesizing advanced materials, including Ti based alloys.[4,5] Titanium and some of its alloys are among the key advanced materials due to the excellent combination of good corrosion resistance, outstanding biocompatibility, and high strength-to-weight ratio; thus, providing a promising candidate for their applications in automotive, aerospace, biomedical implant materials, *etc.*[6,7]

MA proceeds by the continual cold welding and fracturing of the constituent powder particles when repeatedly subjected to high-energy collision of the milling media. The cold welding and fracturing process deform the particles, creating atomically clean surfaces with minimized diffusion distance.[8] However, the balance between welding and fracture may not be achieved in most cases by MA itself, and the tendency for powders to weld together into larger particles predominates and suppresses the process of alloying. It thus becomes imperative to strike a balance between welding and fracture in a MA process so as to develop the desired fine microstructure and intimate alloying. Organic surfactants, generally known as process control agent (PCA), are often used during MA to obtain the critical balance between cold welding and fracture and enhance the process efficiency.[2,8,9] During the MA process, the PCAs are absorbed onto the surface of the particles, inhibiting excessive cold welding by lowering the surface tension of the solid materials. Among the most commonly used PCAs in the MA process are stearic acid (SA)[10,11] and ethylene-bis-stearamide (EBS).[12–14]

Although a number of investigations have studied the effect of PCA on the microstructure, morphology, and thermal properties of powders after MA,[10,13,15–21] little attention has so far been given to the understanding of the microstructure of bulk sintered alloys and to the establishment of a link between the microstructures and the different contents of the PCA. The present study aims to investigate the effect of different SA and EBS additions on the microstructural evolution of powder and bulk sintered biocompatible Ti-16Sn-4Nb (wt pct,

ALIREZA NOURI, Postdoctoral Researcher, PETER D. HODGSON, Professor and Director, and CUI'E WEN, Associate Professor, are with the Institute for Technology Research & Innovation, Deakin University, Waurn Ponds, Victoria 3217, Australia. Contact e-mail: cuie.wen@deakin.edu.au
Manuscript submitted June 1, 2009.
Article published online April 17, 2010

hereafter) alloy for a relatively short period of ball milling time of 5 hours.

II. EXPERIMENTAL PROCEDURE

Elemental metal powders of Ti, Sn, and Nb with particle size of –325 mesh (≤45 μm) and purity of 99.9, 99.9, and 99.8 pct, respectively, were mixed together to give the nominal compositions of Ti-16Sn-4Nb alloy. The MA process was performed in a planetary ball mill (RETSCH PM400, Haan, Germany) using steel balls and zirconia containers at room temperature. The ball-to-powder weight ratio was maintained at 10:1 and the ball milling rotation rate was 200 rpm. SA and EBS were separately added into the containers in the amounts of 1, 2, and 3 pct (wt pct, hereafter) prior to milling, and each batch was run for 5 hours. The typical properties of SA and EBS are presented in Table I. One batch was also run without using PCA, to provide a baseline for comparison. The containers were loaded with the desired compositions and subsequently sealed in a glove box chamber under an atmosphere of argon. The powders in the sealed containers were then ball milled without any further purging with argon. After each run, the containers were transferred to the argon-filled glove box where the ball milled powders were removed and collected for further study. The weight of the powder recovered from the containers was measured after each run. The ball milled powders with different amounts of SA and EBS were consolidated by a uniaxial cold press under the pressure of 500 MPa for 5 minutes. The green compacts were then sintered in a high vacuum furnace at 1473 K (1200 °C) for 3 hours with heating/cooling rate of 10 °C/min.

To observe the microstructure of the as-sintered bulk alloy with the addition of different SA and EBS contents, the specimens were ground and polished *via* conventional metallographic techniques and subsequently etched with Kroll reagent: 3 mL HF, 6 mL HNO_3, and 100 mL H_2O. The particle morphology, microstructures, and distribution of elements within the particles were examined using optical microscopy and scanning electron microscopy combined with backscattered electron imaging (SEM-BEI) and energy-dispersive spectrometry (EDS) (LEICA S440, Cambridge, UK). The chemical analysis of the bulk specimens after sintering was carried out using the inductively coupled plasma–atomic emission spectroscopy (ICP-AES) and LECO* combustion methods. Samples of each powder and bulk material were characterized by X-ray diffraction (XRD) using Cu K_α radiation (35 kV, 28 mA) at a scanning rate of 1 deg/min using a PHILIPS** PW1820 diffractometer.

*LECO is a trademark of LECO Corporation, St. Joseph, MI.

**PHILIPS is a trademark of FEI Company, Hillsboro, OR.

III. RESULTS

A. *Alloying Process*

The alloying process can be followed by observing the microstructural evolution of the powders after the MA process. Figure 1 shows the SEM backscattered electron images of the cross section of the Ti-16Sn-4Nb alloy particles ball milled for 5 hours with the addition of different SA and EBS contents. Obviously, the particles with a small PCA content are larger than those of the powders ball milled with a higher PCA content, as shown in Figures 1(a) and (d), suggesting the dominance of cold welding over fracturing of the particles. These larger powder particles are distinguished by a lamellar-like structure with unalloyed embedded particles. In the previous study,[10] the EDS analysis demonstrated that the bright areas are either Sn or Nb, while Ti particles are presented by the gray areas.

Upon increasing the SA and EBS contents to 2 pct, the entire powder charge changed into a mixture of elongated and equiaxed particle shapes, as shown in Figures 1(b) and (e). At this stage, the microstructure became more heterogeneous with isolated areas of unprocessed materials. However, the fraction of elongated particles and individual particles of Ti, Sn, and Nb for the samples with the addition of 2 pct EBS was greater than that of the samples with the addition of SA. As the SA and EBS contents increased to 3 pct, the majority of the particles remained unalloyed and deformed to either a big elongated shape or progressively fine particles, as shown in Figures 1(c) and (f).

Figure 1(g) shows the microstructure of the powder particles ball milled without the addition of the PCA. This microstructure is represented by a characteristic folded lamellar-like microstructure of Ti, Sn, and Nb layers in each particle. Compared to the powders ball milled with 1 pct SA or EBS, the powder mixture without the addition of the PCA exhibited coarser interfacial boundaries.

B. *Chemical Analysis*

Chemical analysis was conducted to determine the presence of contaminants that may generate from either SA and EBS or the ball milling media. The content of

Table I. Typical Properties of SA and EBS[8]

Generic Name	Chemical Formula	Melting Point	Boiling Point
SA	$CH_3(CH_2)_{16}COOH$	340 to 342 K (67 to 69 °C)	456 to 457 K (183 to 184 °C)
EBS	$[CONHCH_2CH_3(CH_2)_{16}]_2$	413 to 419 K (140 to 146 °C)	532 K (259 °C)

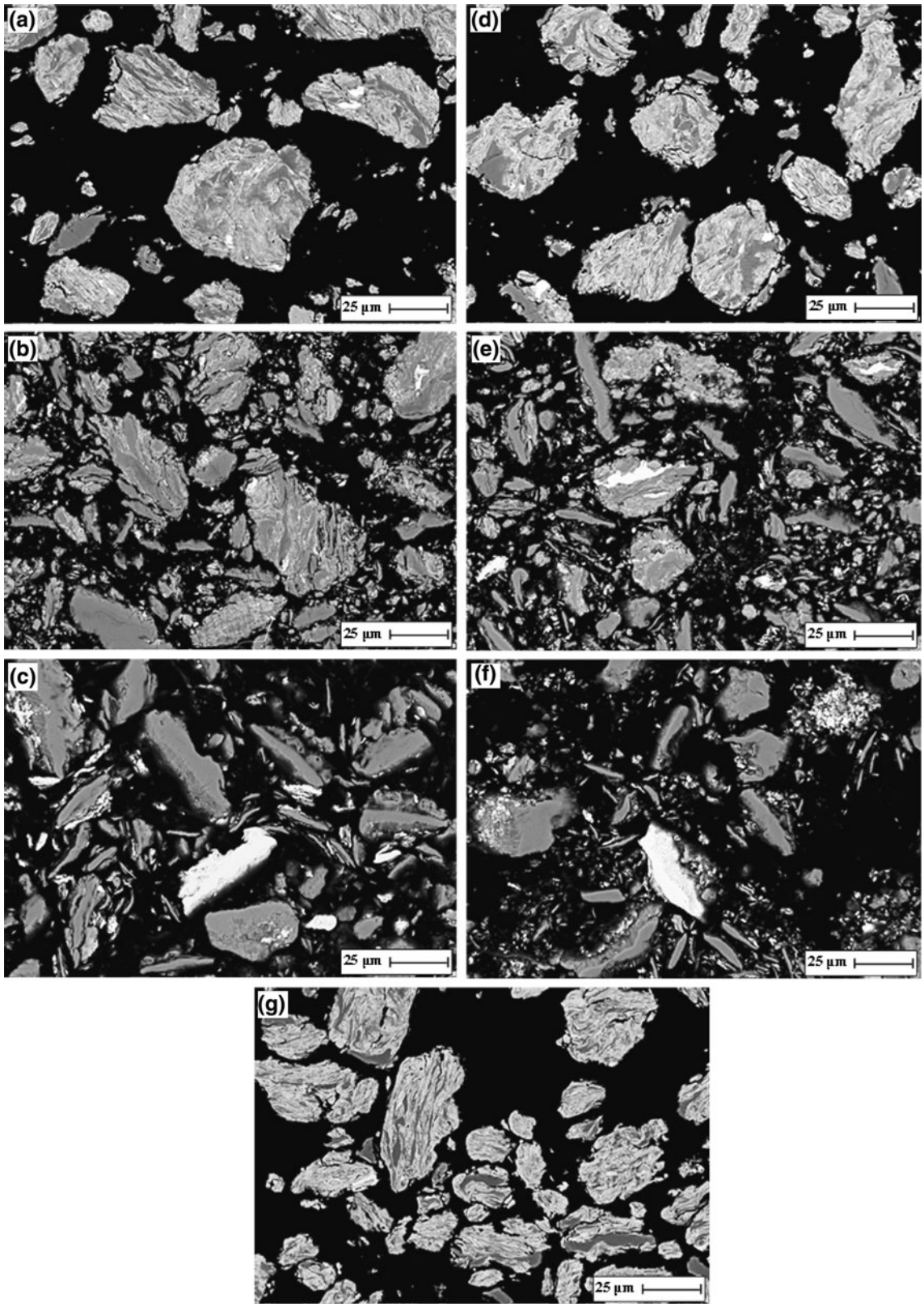

Fig. 1—SEM backscattered electron images of cross section of the Ti-16Sn-4Nb particles ball milled for 5 h with the addition of different PCA contents: (*a*) 1 pct SA, (*b*) 2 pct SA, (*c*) 3 pct SA, (*d*) 1 pct EBS, (*e*) 2 pct EBS, (*f*) 3 pct EBS, and (*g*) non-PCA.

contamination in the bulk sintered Ti-16Sn-4Nb alloy is given in Table II. It is clear that the addition of SA and EBS resulted in appreciable amounts of carbon (C) and oxygen (O) in the bulk sintered samples. However, the content of contamination was more pronounced when EBS was used during the ball milling process.

Meanwhile, the powders ball milled with the addition of 2 pct SA or EBS revealed a higher level of C and O contamination. Large amounts of Fe and Cr were also introduced into the charge when a higher content of PCA was used. As expected, the lowest contaminations corresponded to the sample without the addition of PCA.

C. *Phase Formation*

To understand the phase formation upon the addition of different SA and EBS contents, XRD analysis was carried out on both the powder mixture and the bulk sintered samples. The XRD patterns of the Ti-16Sn-4Nb powder mixtures ball milled for 5 hours with the addition of different SA and EBS contents are shown in Figure 2. The original powder mixture comprised of all elemental metals of Ti, Sn, and Nb (Figure 2(a)). The diffraction patterns of the ball milled powders without the addition of PCA become slightly broader and of less intensity, as shown in Figure 2(b), while the peak intensity of the elemental metals for those of the powders ball milled with 3 pct SA or EBS has the most intense diffraction peaks (Figures 2(e) and (h)). Comparatively, the powders ball milled with the addition of EBS showed slightly sharper diffraction peaks than those of the powders milled with the addition of SA. Meanwhile, the diffraction peaks belonging to Sn and Nb were still detectable in the samples with the addition of 2 and 3 pct PCA, suggesting that Sn and Nb still remained unalloyed after ball milling for 5 hours.

It was noted that the peak positions of Ti slightly shifted to a higher angle when no or 1 pct PCA were used. In the powders ball milled with the addition of 2 pct SA or EBS, the appearance of a new diffraction peak attributable to iron-chromium carbide (FeCrC) was noted, as seen in Figures 2(d) and (g). Irrespective of a slight difference in peak intensities, the powders ball milled with the same amount of SA or EBS appeared to have similar patterns.

The XRD patterns for the bulk sintered Ti-16Sn-4Nb alloy samples with the addition of different SA and EBS contents are shown in Figure 3. As indicated in Figures 3 (b) and (c), only the bulk samples made from the non-PCA and 1 pct SA powder mixtures consist of β-Ti phase. By increasing the content of SA to 3 pct, the β-Ti peak gradually merged into a single α-Ti peak, as shown in Figures 3 (d) and (e). The bulk samples made from the powders ball milled with the addition of 1 pct EBS, however, exhibited an asymmetric peak with

Table II. Contamination Contents of Bulk Ti-16Sn-4Nb Alloy Made from the Powders Ball Milled with Various Amounts of PCA

	Contamination Content (Wt Pct)				
Specimen	O	N	C	Fe	Cr
Non-PCA	0.30	0.01	0.11	0.32	0.07
1 pct SA	0.87	0.01	0.78	0.52	0.12
2 pct SA	1.50	0.01	1.44	1.24	0.18
3 pct SA	1.80	0.01	1.14	1.56	0.28
1 pct EBS	1.45	0.01	1.02	0.71	0.14
2 pct EBS	3.10	0.01	1.28	1.30	0.22
3 pct EBS	2.30	0.01	1.34	2.30	0.44

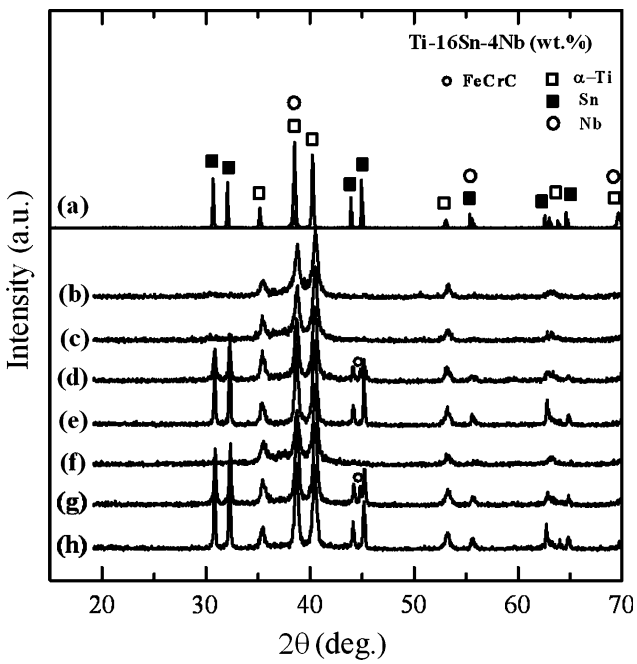

Fig. 2—XRD patterns of (*a*) elemental powders and the Ti-16Sn-4Nb powders ball milled for 5 h with the addition of different PCA contents: (*b*) non-PCA, (*c*) 1 pct SA, (*d*) 2 pct SA, (*e*) 3 pct SA, (*f*) 1 pct EBS, (*g*) 2 pct EBS, and (*h*) 3 pct EBS.

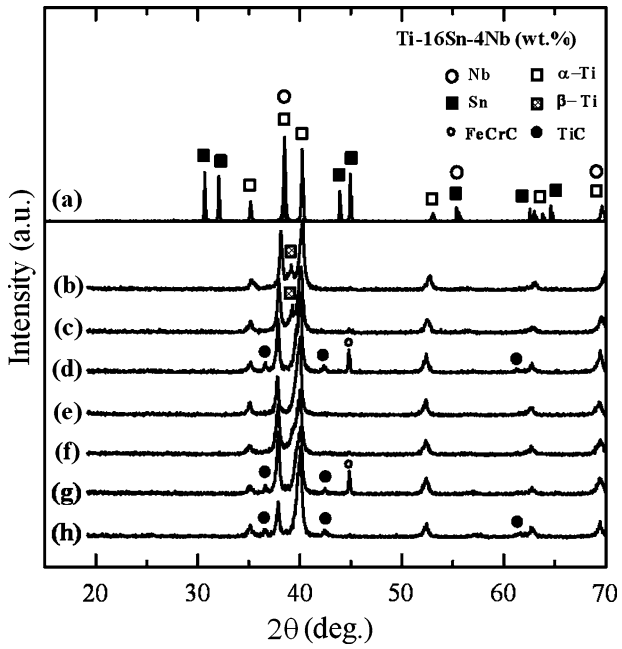

Fig. 3—XRD patterns of (*a*) elemental powders and the bulk Ti-16Sn-4Nb made from the powders ball milled for 5 h with the addition of different PCA contents: (*b*) non-PCA, (*c*) 1 pct SA, (*d*) 2 pct SA, (*e*) 3 pct SA, (*f*) 1 pct EBS, (*g*) 2 pct EBS, and (*h*) 3 pct EBS.

shoulders evident on the high 2θ side (Figure 3(f)). At this stage, the presence of the β-Ti phase is undetectable. Larger amounts of EBS resulted in the progressive disappearance of the β-Ti peak, as shown in Figures 3(g) and (h).

The appearance of new diffraction peaks in the bulk samples made from powders with the addition of 2 pct SA as well as 2 and 3 pct EBS indicated the formation of titanium carbide (TiC), as seen in Figures 3 (d), (g), and (h), respectively. Furthermore, the results indicated the formation of a new peak in the bulk samples when 2 pct SA or EBS were added to the powder mixture during ball milling (Figures 3(d) and (g)). The new peaks were attributable to FeCrC.

D. *Microstructural Characteristics*

1. *Optical microscopy observation*

The microstructures of the bulk sintered Ti-16Sn-4Nb alloy made from the powders ball milled for 5 hours with various SA and EBS contents are presented in Figure 4. The micrographs were taken at magnification of 50 times. Microstructural observation of the bulk samples at room temperature revealed two distinctive areas of the α-Ti matrix and inhomogeneously distributed Nb-rich colonies. The size and volume fraction of Nb-rich colonies in the alloy increased with increasing PCA content. According to the XRD results, the colonies in both samples made from the powders without the addition of PCA or with 1 pct SA can be identified as β-Ti phase.

The microstructure of the bulk sintered samples made from the powders ball milled with SA or EBS did not differ noticeably. However, the microstructure of the samples added with SA provided moderately larger colonies than those added with EBS.

2. *BEI and EDS analyses*

The BEI images of the bulk Ti-16Sn-4Nb alloy made from the powders with various SA and EBS contents are shown in Figure 5 (2000 times magnification). Similar to the optical micrographs, the size and volume fraction of the colonies, seen as bright areas, increased with increasing SA and EBS content. Another clear feature was the high volume fraction of porosities in the samples made from the powders without the addition of PCA and 1 pct PCA (Figures 5(a), (d), and (g)). The higher contents of SA or EBS (2 and 3 pct) led to the formation of particles with curved edges in the bulk samples, as shown in dark color in Figures 5(b), (c), (e), and (f). These particles were mostly distributed in the vicinity of the interphase boundaries with an average diameter of about 5 μm. Furthermore, the volume fraction of particles in the samples made from the powders with the addition of 2 and 3 pct EBS was larger than that of the samples with SA, as shown in Figures 5(b), (c), (e), and (f).

In order to characterize the elemental composition of the bulk sintered samples, EDS analysis was carried out in three different areas as indicated in Figure 5(c). The intensity of X-ray emission of the elemental constituents is shown in Figure 6. The analysis made in the large gray area, indicated as "A" in Figure 5(c), showed a more homogenous contribution of the alloy compositions, which was characterized as α-Ti phase (Figure 6(a)). The EDS spectra of the brighter areas, as seen in Figure 6(b), were comprised of larger amounts of Nb as well as Fe and Cr from the abrasion of the milling tools. Figure 6(c) shows the EDS spectra of the dark particles, depicted as "C" in Figure 5(c). The analysis revealed a strong presence of Ti peaks in the dark particles.

Considering the presence of the TiC diffraction peaks in the samples made from the powders with the addition of high PCA contents (Figures 3(d), (g), and (h)), it is suggested that the particles were TiC. The SEI micrograph of the TiC particles at a higher magnification (10,000 times) is shown in Figure 7.

E. *Powder Yield*

Powder yield is the amount of powder recovered from the container after the ball milling process. The weight of the recovered Ti-16Sn-4Nb alloy powder after ball milling for 5 hours with the addition of different PCA contents is shown in Figure 8. The powder yield showed an upward trend upon increasing the PCA content. In other words, the amount of powder that stuck to the balls and container decreased when larger quantities of PCA were used. The weight recovered from the ball milled powders with 1 pct SA and 1 pct EBS was about 73 and 80 pct, respectively, while only 65 pct of powders were collected from the non-PCA batch. The yield increased to 85 pct using 2 pct SA, whereas the powder mixture with 2 pct EBS showed a higher recovery of 90 pct. Addition of 3 pct SA resulted in higher powder yields of 88 pct. Meanwhile, for the powders ball milled with 3 pct EBS addition, nearly all powders were recovered.

IV. DISCUSSION

A. *Chemistry of PCA*

Principally, the efficiency of a PCA is influenced by its molecular formula. PCAs are mostly organic compounds with amphiphilic molecules, possessing both hydrophilic (polar) and hydrophobic (nonpolar) properties. Figure 9 shows the molecular structure of the SA and EBS used as PCA in the present study. The long hydrophobic tails are comprised of hydrocarbon chains and the hydrophilic heads are made up of methyl groups. The hydrocarbon chain is flexible and can roll up into a ball or stretch out into a long zigzag. Upon using PCAs in the MA process, the hydrophilic heads of the PCA molecules are adsorbed onto the surface of the metal powder thereby lowering the surface tension of the solid material. As a result, the molecules form a monolayer on the surface of the metal powder with their heads sticking into the metal powder and their hydrophobic tails sticking up above the surface of the metal powder. This process would prevent surface contact between metal particles. The better the PCA coverage on the surface of the metal powder, the lower the surface tension achieved, which indeed shows the higher lubricating ability of the PCA.

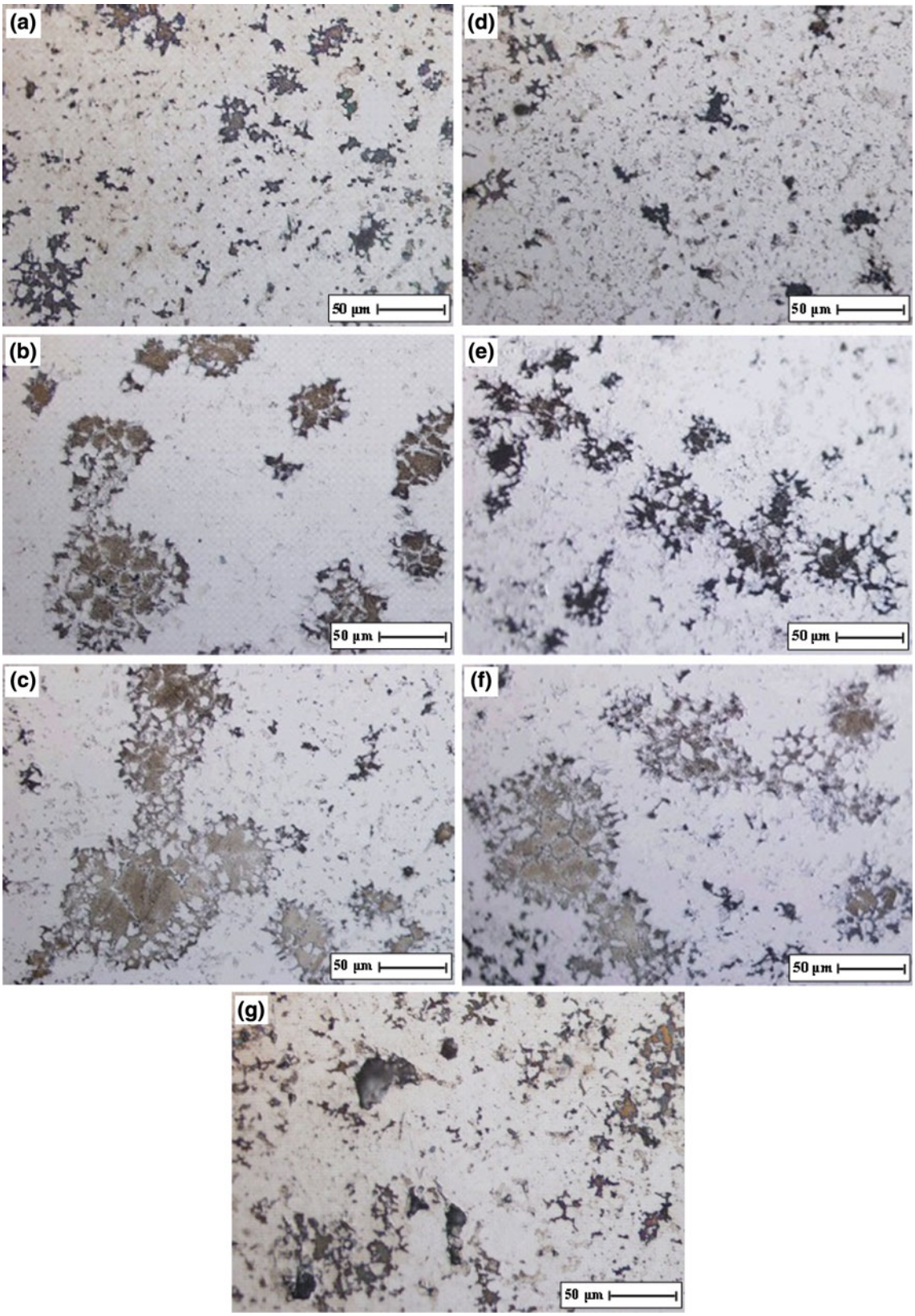

Fig. 4—Optical micrographs of the bulk Ti-16Sn-4Nb alloy made from the powders ball milled for 5 h with the addition of different PCA contents: (*a*) 1 pct SA, (*b*) 2 pct SA, (*c*) 3 pct SA, (*d*) 1 pct EBS, (*e*) 2 pct EBS, (*f*) 3 pct EBS, and (*g*) non-PCA.

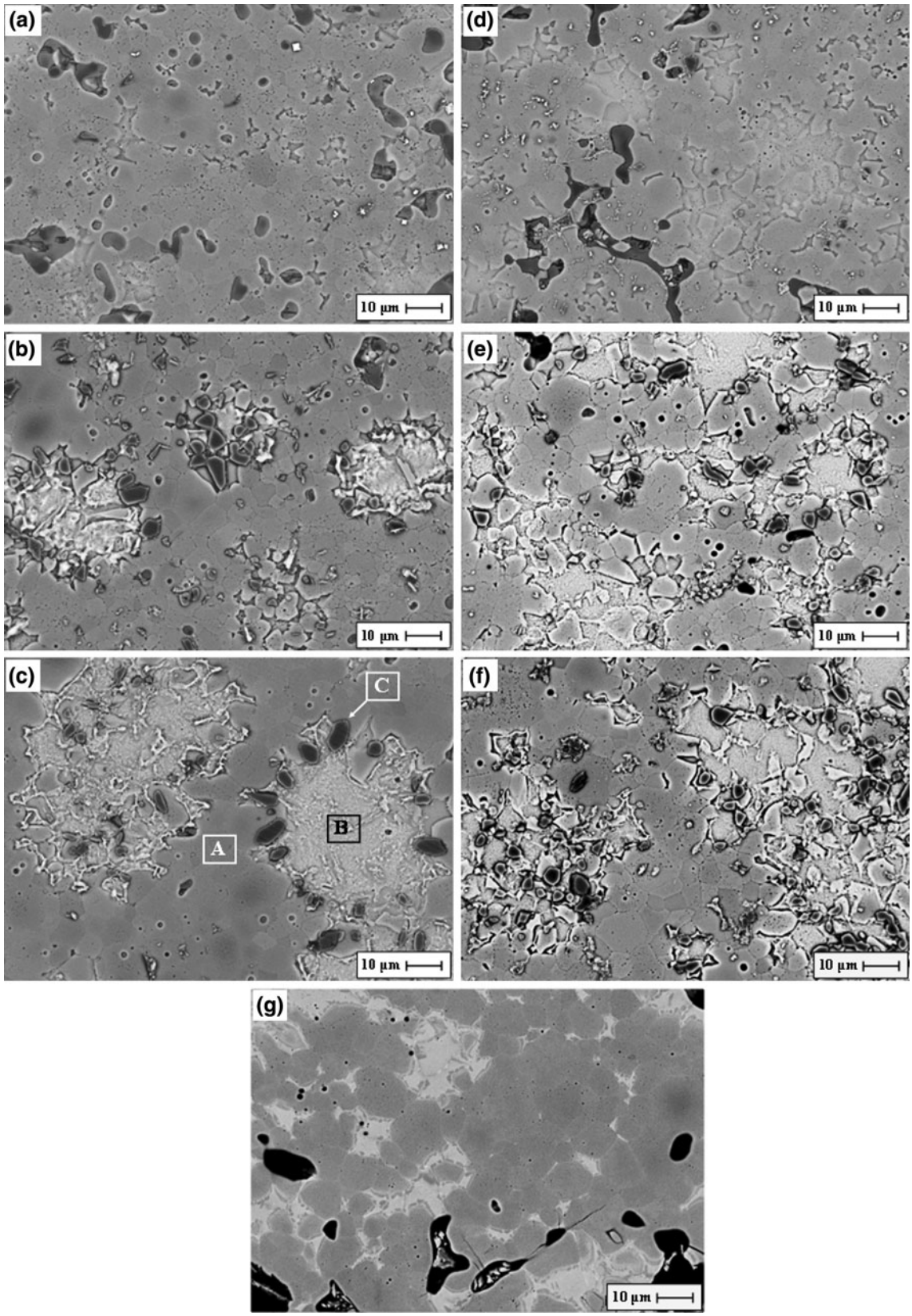

Fig. 5—SEM backscattered images of the bulk Ti-16Sn-4Nb alloy made from the powders ball milled for 5 hours with the addition of different PCA contents: (*a*) 1 pct SA, (*b*) 2 pct SA, (*c*) 3 pct SA, (*d*) 1 pct EBS, (*e*) 2 pct EBS, (*f*) 3 pct EBS, and (*g*) non-PCA.

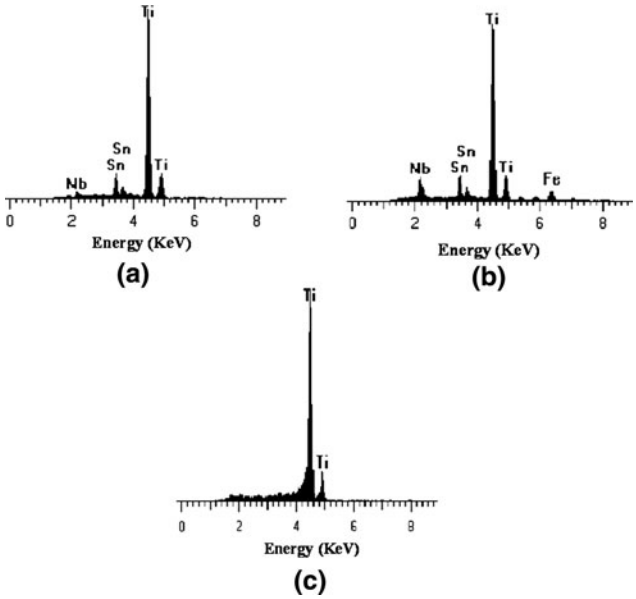

Fig. 6—EDS microchemical analysis of the bulk Ti-16Sn-4Nb alloy made from the powders ball milled for 5 h with the addition of 3 pct SA at three different locations, as indicated in Fig. 5(c).

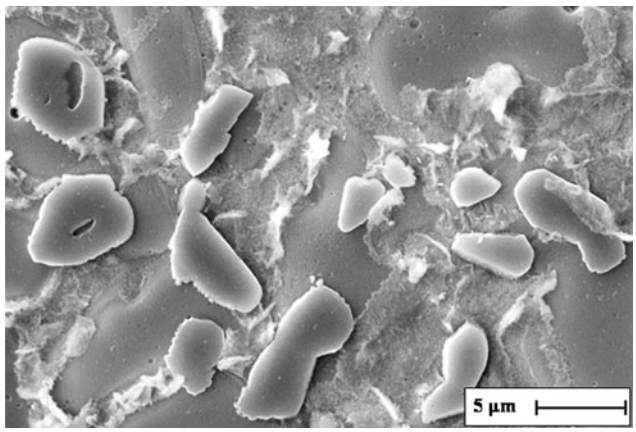

Fig. 7—SEM micrograph of the bulk Ti-16Sn-4Nb alloy made from the powders ball milled for 5 h with the addition of 3 pct EBS showing the distribution of TiC particles in the matrix.

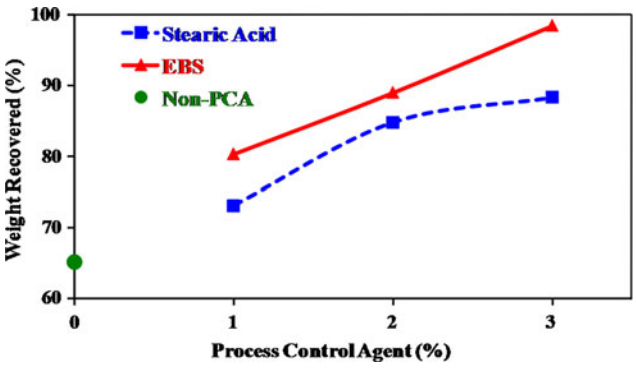

Fig. 8—Amount of powder recovered from the ball milling container with different PCA contents.

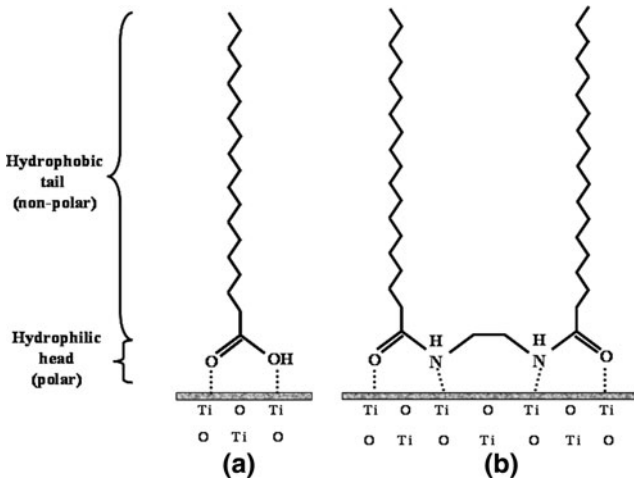

Fig. 9—Schematic illustration of the possible adsorption model for (*a*) SA and (*b*) EBS on the Ti alloy surface.

SA and EBS are typical examples of fatty acids with long hydrocarbon chains containing a methyl group at the end. SA is a monomeric surfactant having one hydrophilic head and one hydrophobic tail, while EBS is a dimeric surfactant made up of two identical amphiphilic moieties, possessing the structure of conventional (monomeric) surfactants connected by a spacer group.[22] However, SA and EBS have different groups at the other end, namely, carboxyl (-COOH) and amide ($-N^{+}(R)_2O^{-}$), respectively.

The different effect of SA and EBS on the ball milled powders can be attributed to the relative sizes and shapes of their hydrophobic and hydrophilic groups.[22,23] In the EBS molecular structure, the presence of the two long hydrophobic tails could give rise to the higher effectiveness of the surfactant, as indicated by the higher powder yield for the powder ball milled with EBS compared to that with SA. The size and shape of the hydrophilic head of EBS may lead to a stronger interaction of the hydrophilic head with the metal surface.

B. *Morphological and Microstructural Characteristics of Ball Milled Particles*

The change in morphology of the powder particles with larger SA and EBS contents can be attributed to the following reasons: (1) a lower rate of cold welding and (2) a microforging process due to the lubricating effect of both SA and EBS. A certain amount of the PCA impedes the fresh metal-to-metal contact by being adsorbed onto the whole surface area of the particles, resulting in the suppression of cold welding and an increase in fracturing rate between the individual particles and the milling tools. By increasing the amount of PCA, deformation occurs primarily in a way that results in flattening of the powder particles. The lubricating effect of the PCA lowers the friction between the colliding balls and particles; thus, the kinetic energy of the colliding balls will repeatedly be used in overcoming the friction force thereby making thin flake particles slide laterally with ease during collision.[15]

It is possible that by continuation of the ball milling process, the large flaky particles become harder and thereby cannot withstand further deformation when collided by the steel balls. The resultant flaky particles may fracture into finer particles by a progressive deformation process. The fracture is facilitated by the propagation of cracks and defects in the particles. However, the ball milling time at this stage is too short to fracture all flakes and achieve a homogenous distribution of fine particles. Therefore, it is further anticipated that with longer ball milling times, the entire flake particles are fractured into smaller particle sizes and a more uniform distribution of the particles is achieved.

For the samples without the addition of a PCA or with 1 pct PCA, however, more direct contact between the particles takes place. The larger equiaxed shape for the particle ball milled with the addition of SA compared to the particle with EBS is attributed to the difference in ratio of O to C in the chemical formula of SA and EBS (SA: 0.15, EBS: 0.07).[9] In this respect, the increase of the ratio of O to C would lead to a larger particle size with more equiaxed shape.

In the MA process, PCA certainly plays a very important role in alloy formation of the elemental powders. In general, the formation of new alloys during MA is highly dependent on the interdiffusion mechanism between constituent alloying elements. The dissolution of solute elements throughout the powder particle matrix is facilitated when diffusion distances are decreased, lattice defect density is increased, and heat is raised.[2,8]

Although the fine and flattened particles obtained with larger PCA contents could provide more free surfaces for alloying, the excessive use of the PCA prevents the formation of new materials. Previous studies have also addressed the delay in the alloying process using different types of PCA.[15,18,24] In the present study, no alloying could be observed when the MA was processed with 3 pct SA or EBS for 5 hours, as shown in Figures 1(c) and (f). This fact is due to the reduction in surface tension of the solid materials by absorption of the PCA, leading to a lower degree of cold welding. On the other hand, the PCA acts as a physical barrier and increases the interdiffusion distance between powder particles, making the particles incapable of contacting each other with fresh surfaces; thus, atoms cannot be transferred through one surface of a particle to another. According to Rocha *et al.*,[18] the PCA could also absorb part of the energy induced by the colliding balls and suppress the cold welding mechanism.

In the absence of the PCA, too much cold welding would lead to an increase in particle size and decrease in interdiffusion between particles. The reduced interdiffusion is manifested by slightly coarser composite layers of Ti, Sn, and Nb built up in the powders without the addition of a PCA, compared to that of fine lamellar structures with 1 pct SA or EBS, as shown in Figures 1(a), (d), and (g). Lu and Zhang[10] have suggested that in ball collisions, the impact energy per unit volume may be reduced by large clusters of large particles; therefore, lower energy can be transferred to the powder particles. Thus, at a given ball milling time, a small amount of the PCA is required for the successful alloying of Ti-16Sn-4Nb alloy and to prevent excessive cold welding.

Another indicator used to measure the degree of cold welding and effectiveness of the PCA, known as powder yield, is the weight fraction of powder collected from the ball milling container after the MA process. The powder yield can be affected by many variables including the intensity of milling, material composition, milling atmosphere, and temperature of milling.[2] One of the main advantages of using PCAs is to improve the powder yield that further reduces the processing cost. Zhang *et al.*[16] showed that using 0.5 to 4 pct SA or polyethylene glycol as the PCA increased the weight fraction of magnesium recovered after ball milling. In another study by Lu and Zhang,[10] a total of 1, 2, and 4 pct SA were used in the ball milling process, and the effect of the PCA on the weight recovered after different ball milling times was also investigated. The powder yields for those powders ball milled with the addition of 2 and 4 pct SA were virtually the same, showing the full recovery at different ball milling times, while the recovered weight dramatically decreased after 5 hours of ball milling for those powders with 1 pct SA or EBS.

In principle, the amount of powder recovered from the ball milling container can determine the effectiveness of the PCA. In the present study, the larger amounts of powder yield for the powders added with EBS compared to the powders added with SA are indicative of the higher effectiveness of the EBS. Although PCAs are employed to minimize cold welding and to increase the powder yield, they become incorporated in the form of inclusions or dispersoids into the powder particles and can alter the nature of the ball milling product. Therefore, a trade-off should be made to maintain high the powder yield and the purity of the powder.

The type of PCA and its content also have considerable effects on the microstructural evolution of the bulk sintered alloy. Essentially, the microstructure of the as-sintered bulk alloy is affected by the morphology and microstructure of its constituent powder particles. As previously described in the alloying process, the solute elements of Sn and Nb are incorporated within the Ti matrix, forming a characteristic folded lamellar-like microstructure. The size of the resulting Nb-rich colonies in the as-sintered bulk samples is approximately proportional to the size of the lamellar layers (especially Nb) in the powder particles. Similarly, the large unalloyed solute particles in a high PCA content give rise to large colonies in the obtained bulk samples. In consequence, the relatively larger size of Nb-rich colonies was more noticeable for the samples made from the powders with SA than that of the samples with EBS. The effect of both SA and EBS addition on the microstructural evolution of the bulk Ti-16Sn-4Nb is schematically illustrated in Figure 10.

The SEM-BEI micrographs of the bulk alloys made from the powders with the addition of larger contents of 2 and 3 pct SA or EBS showed the presence of micron-sized TiC particles. Most of these particles are located along the interphase boundaries, as seen in black color in Figure 5. At high temperatures, the diffusivity of the

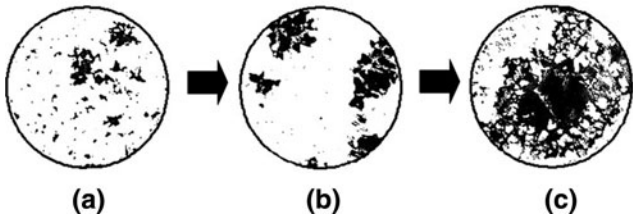

Fig. 10—Schematics of microstructural evolution of the bulk Ti-16Sn-4Nb with the addition of different PCA contents: (*a*) 1 pct, (*b*) 2 pct, and (*c*) 3 pct.

C atoms is enhanced, leading to rapid nucleation on sites near the grain boundaries or interphase boundaries due to their high energy state.[25,26] According to the literature, TiC has a NaCl type crystal structure and can take on an equiaxed shape with curved edges.[27,28] Using metallographic techniques, the TiC particles can be seen as islands standing out against the Ti matrix background and are in very slight relief on the surface.[29]

The EDS analysis also revealed the presence of Fe and Cr peaks in the bright Nb-rich colonies. Similar to Nb, Fe and Cr are β stabilizing elements and have higher solubility in β-Ti (Nb-rich colonies) than in α-Ti.[30]

C. *XRD Analysis and Contamination Level of the Powder and Bulk Sintered Samples*

The high level of contamination in the bulk Ti-16Sn-4Nb alloy after sintering can primarily be attributed to the addition of both SA and EBS to the powder mixture as well as the wear of the milling tools during the ball milling process. The SA and EBS used as PCA in this study have relatively low melting and boiling points and decompose into hydrogen, O, and C due to the rise in temperature during the MA process.

It has been known that the MA process is accompanied by the wear of the grinding media, particularly in high energy ball mills. For instance, milling of prealloyed Al-Cu-Fe powder after 300 hours introduced 1.2 at. pct Fe and very little of other elements.[31] The contamination from milling tools (*i.e.*, Fe and Cr) has been reported to decrease with an increasing amount of PCAs.[2,20,32] These results are in contrast to our observations. As listed in Table II, the amounts of Fe and Cr, caused by the wear of the milling tools, are increased with the addition of both SA and EBS.

The ball surface and grinding medium of those batches ball milled without the addition of the PCA or only with the addition of small SA and EBS contents were coated with a moderately thick layer of powders. This coating is believed to be beneficial for preventing the excessive wear of the milling tools, thereby lowering the powder contamination. The cross section of a milling ball after ball milling for 5 hours without the addition of the PCA is shown in Figure 11. However, too much thickness of the coating layer on the inner walls of the milling tools could also lead to a considerably low powder yield and formation of a heterogeneous product.[3]

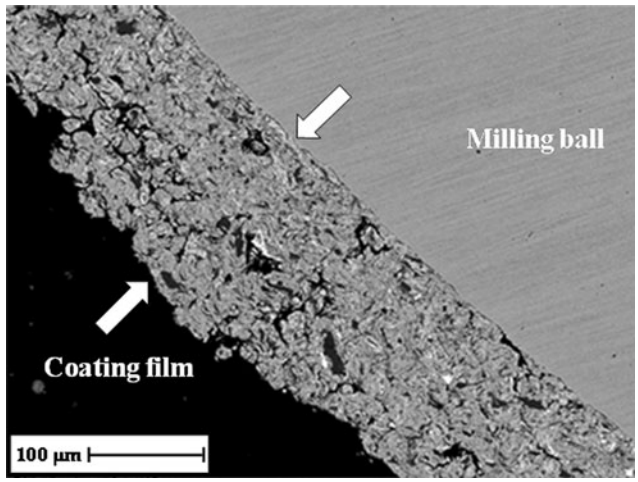

Fig. 11—Cross section of the milling ball after MA for 5 h without the addition of PCA, showing the formation of coating film of Ti-16Sn-4Nb.

In the present study, the C content of the alloy is derived primarily or exclusively from both SA and EBS. Carbon is incorporated into the powder and contributed to the dispersoid content. During the MA process or the subsequent heat treatment, a portion of the C may form carbon dioxide (CO_2) and escape from the system. It has been reported that when an organic PCA such as SA is used in the MA process, carbon monoxide (CO), water vapor, and CO_2 will exist in the milling atmosphere as breakdown products of the PCA.[33]

Since the nitrogen contamination in all batches is negligibly small, it is assumed that a substantial increase in O content in the bulk alloy is not primarily associated with contamination from the milling atmosphere and can be explained by decomposition of the PCA during ball milling as well as further sintering. The level of contamination can also be correlated with the particle size. The smaller particle size and larger surface area give rise to higher contamination values. However, the present study revealed that the use of larger SA or EBS contents did not necessarily result in higher contamination values. For instance, the C contamination showed a higher value when 2 pct SA was used in the powder mixture instead of 3 pct SA. Similarly, the powders ball milled with 2 pct EBS demonstrated a larger amount of O contamination than that with 3 pct EBS (Table II). Kleiner *et al.*[19] observed that for short ball milling times of up to 12 hours, the smaller PCA content would lead to a higher decomposition rate. They suggested that enhanced lubrication in large PCA contents results in reduction of the local temperatures during ball collisions, thereby decreasing the decomposition of the PCA.

In general, the contamination of the powder is more pronounced when higher PCA additions and longer ball milling times are used. In the present study, using 2 or 3 pct SA or EBS in short ball milling times of 5 hours can defeat the purpose of the ball milled powders for making the intended materials.

The alloying process can also be reflected in XRD analysis. The results clearly indicated that the addition of

both SA and EBS caused a delay in the formation of the Ti based solid solution. This is manifested by increasing the intensities of solute diffraction peaks of Sn and Nb with increasing PCA contents from 1 to 3 pct, as shown in Figure 2. In other words, large amounts of the PCA at given ball milling time are inappropriate for the MA process. The slightly sharper diffraction peaks for the powders ball milled with the addition of EBS than those with SA suggest the lower solid solution formation rate in the former. A slight shift in the Ti diffraction peak position of the powder without the addition of the PCA can probably be related to the larger plastic deformation on these powders developed during ball milling. Similarly, the excessive amounts of the PCA in a short ball milling process decrease the friction coefficient between the powder and ball, and enable their sliding over each other with less plastic deformation. The disappearance of the peaks of the alloying elements of Sn and Nb in the sintered bulk samples can be attributed to the formation of a Ti based solid solution, partially during the MA process and partially during the sintering at high temperature.

The presence of the FeCrC diffraction peaks for the samples made from the powders with the addition of 2 pct SA could be correlated with the excess of C decomposed at this stage, as seen in Table II. However, in the case of the sample with 2 pct EBS, no clear conclusion can be drawn from this information. It is unknown whether the larger amount of interstitial contaminants, C and O, in the sample with 2 pct EBS may have accounted for the formation of FeCrC. These peaks become more noticeable for the bulk sintered samples.

The absence of solute peaks in the XRD patterns of bulk alloy is taken as proof of complete solid solution, suggesting the higher diffusion rate of solute elements at a given sintering temperature. The formation of the β-Ti phase is due to the solid solution of the Nb element into Ti matrix. Niobium is a β-Ti stabilizing element and can diffuse into the Ti lattice and form a solid solution during sintering.[6] Since the solution process was controlled by a diffusion mechanism, more β-Ti was obtained when smaller amounts of the PCA were used. The larger PCA content may not only hinder the diffusion process, but also increase the $\alpha \leftrightarrow \beta$ transition temperature by introducing O and C,[30] leading to the disappearance of β-Ti diffraction peaks. In general, the presence of impurities in the alloy can also be detected either by shifts in peak positions or the appearance of new diffraction peaks in the XRD patterns. The former indicates a change in lattice spacing, while the latter is due to the formation of a new phase. Following the addition of the PCA, the Ti crystal lattice would be expected to expand slightly to accommodate the interstitial atoms of O and C, leading to a shift of the Ti diffraction peaks to lower Bragg angles.

The formation of TiC in the samples made from the powders with larger SA and EBS contents is attributed to the decomposition of the PCA into C during the ball milling process. Considering the phase diagrams, the Ti lattice can accommodate significantly less C atoms than other the interstitial elements of O, hydrogen, and nitrogen due to the lower solubility of C in α-Ti.[30,34] As a result, sintering the ball milled powder with the addition of larger PCA contents at high temperature results in the precipitation of TiC within the matrix. Carbon reacts with Ti to form TiC only at a relatively high temperature of above 1273 K (1000 °C). Based on the present results, the TiC diffraction peaks began to appear in the bulk alloy for 2 and 3 pct SA and EBS contents. The disappearance of the TiC peaks in the sample with 3 pct SA is not clear yet. However, the microstructural observation of the same sample by SEM demonstrated the presence of TiC particles in the matrix, implying that the absence of TiC peaks at this stage might not be sufficient evidence for ignoring its presence. No additional diffraction peak related to the existence of new phases was visible.

V. CONCLUSIONS

In the present study, elemental metal powders of Ti, Sn, and Nb were mechanically alloyed in a planetary ball mill for a short period of time of 5 hours. The influence of SA and EBS as PCAs on the characteristics of powder and bulk sintered Ti-16Sn-4Nb (wt pct) alloy was investigated. The conclusions are summarized as follows.

1. The powders ball milled without the addition of SA or EBS or with the addition of 1 pct SA or EBS resulted in rather equiaxed-shape and large particles. By increasing both the SA and EBS contents to 3 pct, the majority of the particles became smaller in size with a flaky-shaped morphology.
2. The microstructural observation of the particles indicated the evolution of a lamellar structure when no PCA or only 1 pct PCA was used in the powder mixture.
3. XRD results and microstructural observation indicated that increasing the SA or EBS contents to 3 pct can drastically suppress the process of alloying. However, an optimum amount of up to 1 pct SA or EBS led to a good balance between the cold welding and fracturing. Alloy formation was more suppressed for the samples ball milled with EBS than that of the samples with SA.
4. The use of a small amount of SA or EBS (1 pct) during the ball milling process led to a microstructure of a homogeneous distribution of fine Nb-rich colonies (β phase) within the α-Ti matrix in the bulk sintered alloy.
5. Addition of both SA and EBS contaminated the resulting bulk alloy with mostly C and O, as well as small amounts of iron and chromium. The formation of TiC was identified for the samples made from the powders ball milled with the addition of 2 and 3 pct SA or EBS contents. Moreover, it appeared that the β-Ti phase decreased with increasing amounts of SA and EBS.

ACKNOWLEDGMENTS

The authors acknowledge the financial support from the VCAMM (Victorian Centre for Advanced Materials Manufacturing) and ARC (Australian Research

Council) through the ARC Discovery Project DP0770021. Peter Hodgson is also supported by the ARC through a Federation Fellowship. The kind assistance from Dr. Andrew Duthie for sample etching is gratefully acknowledged.

REFERENCES

1. D.L. Zhang: *Prog. Mater. Sci.*, 2004, vol. 49, pp. 537–60.
2. C. Suryanarayana: *Prog. Mater. Sci.*, 2001, vol. 46, pp. 1–184.
3. P.S. Gilman and J.S. Benjamin: *Ann. Rev. Mater. Sci.*, 1983, vol. 13, pp. 279–300.
4. C. Suryanarayana and F.H. Froes: *Adv. Mater.*, 1993, vol. 5, pp. 96–106.
5. C.E. Wen, Y. Yamada, and P.D. Hodgson: *Mater. Sci. Eng. C*, 2006, vol. 26, pp. 1439–44.
6. G. Lütjering and J.C. Williams: *Titanium*, Springer-Verlag, Berlin, 2003, pp. 13–50.
7. J.B. Park and R.S. Lakes: *Biomaterials: An Introduction*, Plenum Press, New York, NY, 1994.
8. L. Lü and M.O. Lai: *Mechanical Alloying*, Kluwer Academic Publishers, Boston, MA, 1998.
9. P.R. Soni: *Mechanical Alloying, Fundamentals and Applications*, International Science Publishing, Cambridge, United Kingdom, 1999.
10. L. Lu and Y.F. Zhang: *J. Alloys Compd.*, 1999, vol. 290, pp. 279–83.
11. C.J. Rocha and R.M. Leal Neto: *Mater. Sci. Forum*, 2003, vols. 416–418, pp. 144–49.
12. A. Nouri, X.B. Chen, Y.C. Li, Y. Yamada, P.D. Hodgson, and C.E. Wen: *Mater. Sci. Eng. A*, 2008, vol. 485, pp. 562–70.
13. H.S. Huang, Y.C. Lin, and K.S. Hwang: *Int. J. Refract. Met. Hard Mater.*, 2002, vol. 20, pp. 175–80.
14. P.S. Gilman and W.D. Nix: *Metall. Trans. A*, 1981, vol. 12A, pp. 813–24.
15. L. Shaw, M. Zawrah, J. Villegas, H. Luo, and D. Miracle: *Metall. Mater. Trans. A*, 2003, vol. 34A, pp. 159–70.
16. Y.F. Zhang, L. Lu, and S.M.Yap: *J. Mater. Proc. Technol.*, 1999, vols. 89–90, pp. 260–65.
17. R. Juárez, J.J. Suñol, R. Berlanga, J. Bonastre, and L. Escoda: *J. Alloys Compd.*, 2007, vols. 434–435, pp. 472–76.
18. C.J. Rocha, E.G. de Araujo, R.A. Nogueira, and F. Ambrozio Filho: *Mater. Sci. Forum*, 1999, vols. 299–300, pp. 457–62.
19. S. Kleiner, F. Bertocco, F.A. Khalid, and O. Beffort: *Mater. Chem. Phys.*, 2005, vol. 89, pp. 362–66.
20. A.P. Radlinski, A. Calka, B.W. Ninham, and W.A. Kaczmarek: *Mater. Sci. Eng. A*, 1991, vol. 134, pp. 1346–49.
21. P.B. Joshi, G.R. Marathe, A. Pratap, and V. Kurup: *Hyperfine Interact.*, 2005, vol. 160, pp. 173–80.
22. H. Gecol: in *Chemistry and Technology of Surfactants*, R.J. Farn, ed., Blackwell Science Ltd, Oxford, United Kingdom, 2006, pp. 24–45.
23. S. Gaysinsky, P.M. Davidson, D.J. McClements, and J. Weiss: *Food Biophys.*, 2008, vol. 3, pp. 54–65.
24. P. Bhattacharya, P. Bellon, R.S. Averback, and S.J. Hales: *J. Alloys Compd.*, 2004, vol. 368, pp. 187–96.
25. D.A. Porter and K.E. Easterling: *Phase Transformation in Metals and Alloys*, Chapman and Hall, London, 1992.
26. W.D. Callister: *Materials Science and Engineering: An Introduction*, 4th ed., John Wiley & Sons, Inc., New York, NY, 1997.
27. F.J.J. van Loo and G.E. Bastin: *Metall. Trans. A*, 1989, vol. 20A, pp. 403–11.
28. Z. Yang, W. Lu, J. Qin, and D. Zhang: *Mater. Sci. Eng. A*, 2006, vol. 425, pp. 185–91.
29. X. Yulin: *Met. Powder Rep.*, 2007, vol. 62, pp. 16–18.
30. E.K. Molchanova: *Phase Diagrams of Titanium Alloys (Translation of Atlas Diagram Sostoyaniya Titanovyk Splavov)*, Israel Program for Scientific Translations, Jerusalem, 1965.
31. F.X. Zhang and W.K. Wang: *J. Alloys Compd.*, 1996, vol. 240, pp. 256–60.
32. E. Gaffet, M. Harmelin, and F. Faudot: *J. Alloys Compd.*, 1993, vol. 194, pp. 23–30.
33. A.D. Jatkar, P.S. Gilman, and R.C. Benn: U.S. Patent 4624705, 1986.
34. C.R. Brooks: *Heat Treatment, Structure and Properties of Nonferrous Alloys*, ASM, Metals Park, OH, 1982.